Pulsed laser deposited hard TiC, ZrC, HfC and TaC films on titanium: Hardness and an energy-dispersive X-ray diffraction study

D. Ferro [a], J.V. Rau [a], V. Rossi Albertini [b], A. Generosi [b], R. Teghil [c], S.M. Barinov [d],*

[a] Istituto per lo Studio dei Materiali Nanostrutturati, CNR, Piazzale Aldo Moro 5-00185 Rome, Italy
[b] Istituto di Struttura della Materia, CNR, via del Fosso del Cavaliere, 100-00133 Rome, Italy
[c] Universitá della Basilicata, via N. Sauro 85-85100, Potenza, Italy
[d] Institute for Physical Chemistry of Ceramics, Russian Academy of Sciences, Ozernaya 48, Moscow, 119361, Russia

Abstract

Thin films of TiC, ZrC, HfC and TaC were pulsed laser ablation deposited onto sandblasted pure titanium substrate at a laser beam fluence of 3 J/cm^2. Deposition temperature was room temperature or 500 °C. The films were investigated by scanning electron microscopy, energy-dispersive X-ray diffraction (EDXD) and hardness measurements. The smooth and compact films of 200 to 600 nm thickness were obtained, consisting of tens nanometer particles. The rocking curve EDXD analysis revealed the films are textured. Intrinsic hardness of the films decreases generally with an increase in substrate temperature and in molecular weight of carbides.
© 2007 Elsevier B.V. All rights reserved.

1. Introduction

Titanium and titanium base alloys are widespread in clinical use as implant materials providing a good combination of mechanical properties, corrosion resistance, and biocompatibility [1]. Some titanium implants are intended for long term or permanent location, for example, as orthopaedic joint prostheses. A clinical problem sometimes encountered with titanium implants and their abutments is that they are relatively soft and easy to damage [2]. Another problem to be solved is the protection of titanium against oxidation at the harsh conditions of the body fluids surrounding the implanted device. Transient titanium oxides being formed on titanium surface reduce the wear resistance. A high wear rate may result in wear debris accumulation, adverse cellular response and implant loosening. The addition of thin hard coating to the surface of titanium might overcome those problems, i.e. to protect titanium against oxidation and to improve surface hardness. Therefore, continuous research has been directed towards surface modification of titanium. The most popular approach is to apply calcium phosphate coatings, some recent

results being outlined in [3]. The current method of calcium phosphates depositing, is the plasma-spraying process. Problems with the plasma-sprayed coatings include poor adhesion strength and alterations in both the structure and the phase composition of the film influencing the bioactivity [3,4]. Besides, the mechanical properties of calcium phosphates, such as hardness, are poor to prevent wear. Alternatively, some refractory nitrides and carbides were considered to be good candidatures for the surface modification of titanium implant due to their resistance to oxidation and high hardness. Titanium nitride [5] and titanium carbide [6] were demonstrated to possess a high bioactivity for osteointegration. Otherwise, different bio-inactive refractory carbides might be deposited on titanium surface. In particular, niobium carbide coating was shown to decrease the wear rate of metals [7]. Various physical deposition methods to cover metals with refractory carbide films are being explored [8,9]. Among these, the pulsed laser ablation deposition (PLAD) technique has been successfully employed to deposit thin carbide films on silicon [10–12], providing films of high hardness. A great advantage of PLAD is the conservation of the stoichiometry of virtually any target material in the deposition [13]. The present work is aimed at the PLAD of TiC, ZrC, HfC and TaC films on titanium substrate, varying the substrate preheating temperature,

---

* Corresponding author. Tel.: +7 495 4379892; fax: +7 495 4379893.
E-mail address: barinov_s@mail.ru (S.M. Barinov).
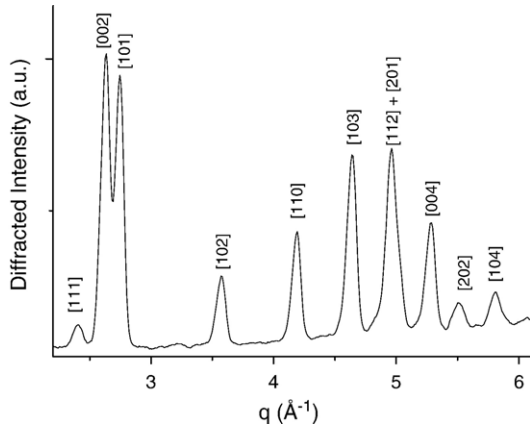
Fig. 1. Diffraction pattern of Ti substrate: [110] at $q=2.455(5)$ Å^{-1}; [002] at $q=2.687$ (5) Å^{-1}; [101] at $q=2.800(5)$ Å^{-1}; [102] at $q=3.658(5)$ Å^{-1}; [110] at $q=4.268$ (5) Å^{-1}; [103] at $q=4.735(5)$ Å^{-1}; [112] and [201] convoled at $q=5.060(5)$ Å^{-1}; [004] at $q=5.375(5)$ Å^{-1}; [202] at $q=5.612(5)$ Å^{-1}; [104] $q=5.929(5)$ Å^{-1}.

which was predicted to affect the film morphology [13] and, therefore, the mechanical properties, i.e. hardness. The films morphology was investigated by the Scanning Electron Microscopy (SEM), their structure was studied by using the energy-dispersive X-ray diffraction (EDXD) method, and the intrinsic

hardness of the films was evaluated by the Vickers microhardness measurements.

2. Materials and methods

2.1. Films deposition

Targets for PLAD were fabricated by using carbide powders (TiC — 98% pure, ZrC — 99% pure, HfC — 98% pure, TaC — 99% pure; Aldrich Chemical Co.) that were hot pressed into 18 mm diameter and 5 mm high pellets. The pure titanium substrates were sandblasted with a 60-grid SiC abrasive to provide surface roughness, R_a, of approximately 1.6 μm. The ablation and deposition experiments were performed by means of the experimental apparatus described in detail elsewhere [14]. It consists of a stainless steel vacuum chamber, evacuated to a pressure of 1.5×10^{-4} Pa, and equipped with a rotating target holder and a heatable substrate support. The distance between the target and the substrate was 20 mm. A frequency-doubled Nd: glass laser (529 nm emission wavelength, 250 fs pulse duration, 10 Hz repetition rate) was used for the ablation and deposition experiments. The laser fluence in our experiments was ∼3.0 J/cm^2 and the laser beam incident at an angle of 45° on the target surface. The deposition time was about 2 h. The Ti substrates were
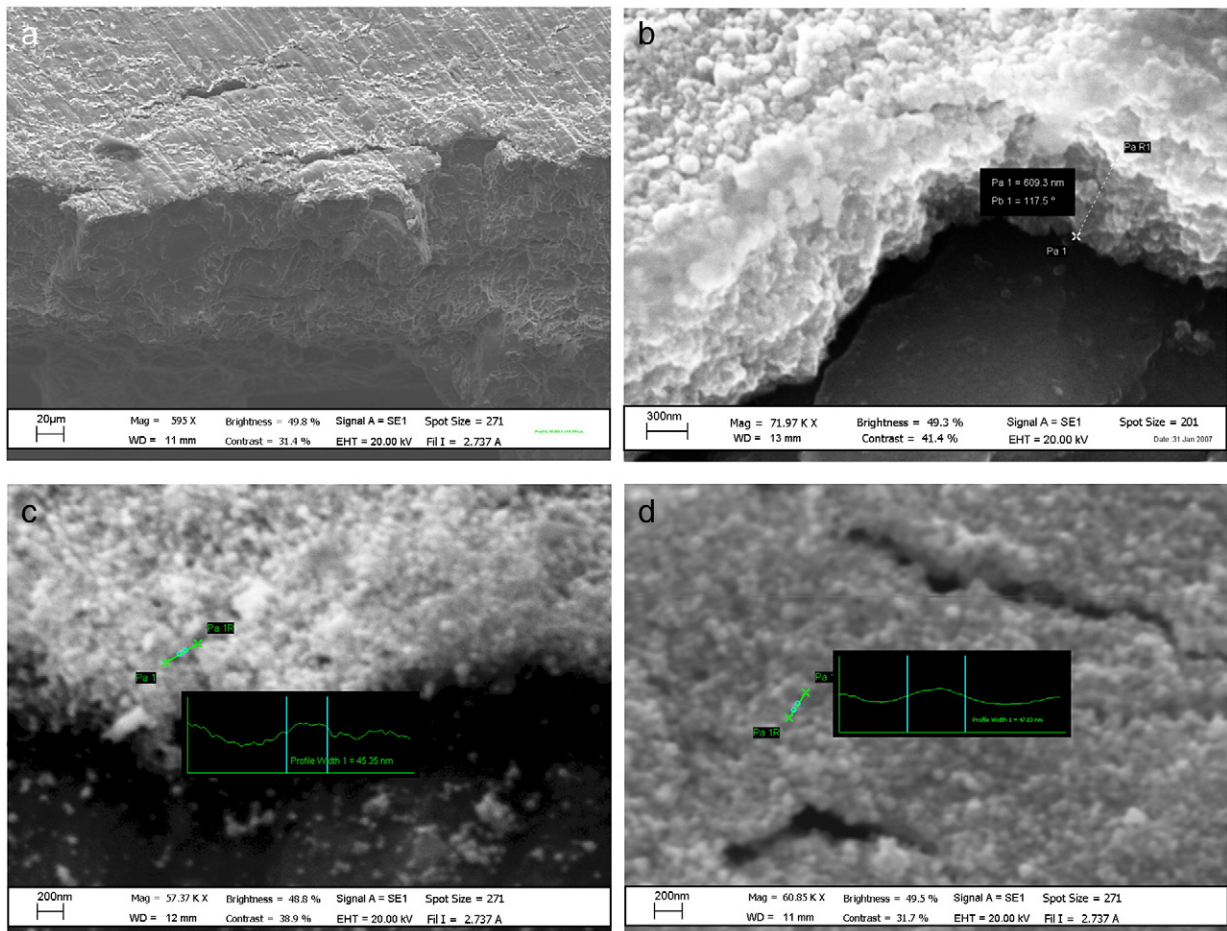
Fig. 2. SEM micrograph of TiC film on Ti substrate deposited at 500 °C (a); ZrC film deposited at room temperature (b); HfC film deposited at room temperature (c), and TaC film deposited at 500 °C (d).

Table 1
Thickness of the films, hardness of films and bulk ceramics

Compound	Thickness, nm		Hardness of film, GPa		Hardness of bulk ceramics, GPa [22]
	Substrate: RT	Substrate: 500 °C	Substrate: RT	Substrate: 500 °C	
TiC	500	330	24±2	23±2	30
ZrC	600	590	20±2	17±3	20–22
HfC	500	220	18±1	18±2	18–20
TaC	250	240	19±3	14±1	14

kept at room temperature and at 500 °C. The preheating temperature was measured with a thermocouple (error±10 °C). The thermocouple is attached to the bottom of the substrate holder. The thickness of the film was evaluated by scanning electron microscopy (SEM, microscope LEO 1450 VP), the absolute error of the thickness measurement being±10 nm.

2.2. EDXD measurements

The EDXD measurements were performed by a non commercial apparatus, based on the use of a non-monochromatized ("white") primary X-ray beam (produced by a W anode) and an ultra pure Ge solid-state detector, which is able not only to count the number of the diffracted photons but also to measure the energy of each of them. In this way, the reciprocal space scan necessary to draw the diffraction pattern, i.e. the scan of the scattering parameter q (where $q = a\,E\,\sin\vartheta$ is the normalized momentum transfer magnitude, a is a constant, E is the energy of the incident X-ray beam and 2ϑ is the scattering angle), is carried out electronically, rather than mechanically as in the ordinary (i.e. Angular Dispersive) X-ray diffraction. This experimental setup was used to perform the
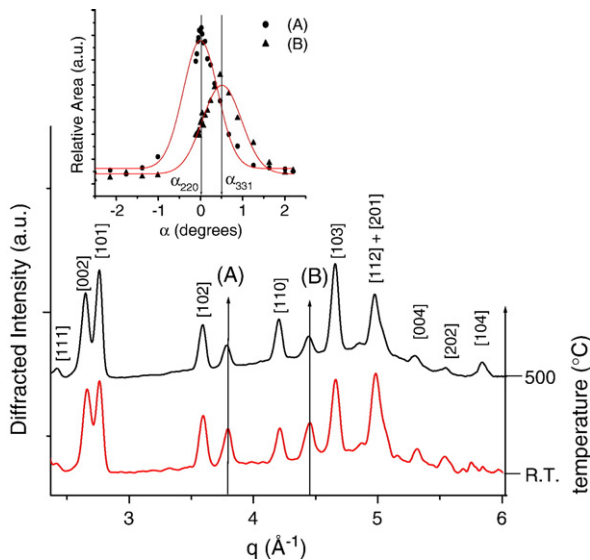
Fig. 3. Diffraction patterns of HfC/Ti, deposited at RT (lower curve) and 500 °C (upper curve) respectively. The Ti reflections are labelled as previously. The arrows indicates (A) HfC [220] reflection at q=3.835 (5) Å^{-1} and (B) HfC [311] reflection at q=4.495 (5) Å^{-1}. In the inset the RC of (A) and (B) are shown and the mismatch, $\triangle\alpha=0.50°$, is evidenced by the different position of the maxima α_{311} and α_{220}.
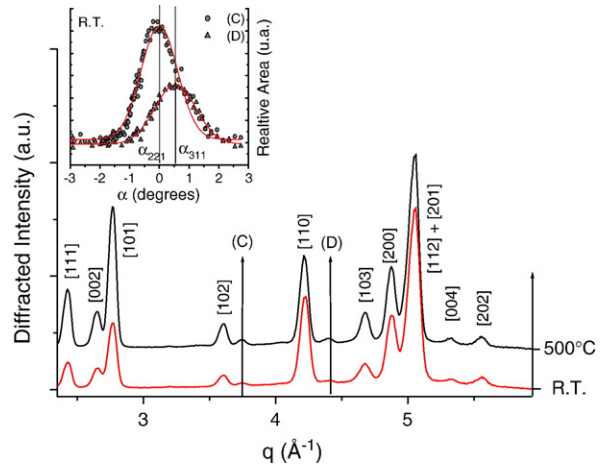
Fig. 4. Diffraction patterns of ZrC/Ti, deposited at RT and 500 °C. The arrows indicates (C) ZrC [220] reflection at q=3.799 (5) Å^{-1} and (D) ZrC [311] reflection at q=4.460 (5) Å^{-1}. In the inset, the RC of (C) and (D) (sample deposited at RT) is shown and the mismatch, $\triangle\alpha=0.51°$, is evidenced by the different position of the maxima α_{311} and α_{220}.

investigation of the structural properties of all the samples, including the measurement of their rocking curves [15,16].

The rocking curve of a polycrystal represents the statistical distribution of the orientation of its crystalline domains. It can be obtained by measuring the intensity variations of a given Bragg peak, as a function of the asymmetry parameter: $\alpha = (\vartheta i - \vartheta r)/2$, where ϑi, ϑr are the incident and reflection angles, respectively, while the total scattering angle $(\vartheta i + \vartheta r) = 2\vartheta$ is kept unchanged. In practice, the rocking curve is calculated by normalizing the intensity of the peak observed at each α-value to the maximum intensity of the peak along the α-scan.

The main advantage of the Energy Dispersive mode over its conventional counterpart in performing X-ray diffraction experiments is that the geometric setup is kept fixed during the acquisition of the diffraction patterns, which simplifies the experimental geometry and prevents systematic angular errors as well as possible misalignments. In particular, the technique provides a faster recording of the Bragg peaks and, consequently, of their rocking curves since, in the ED mode, the whole diffraction pattern is obtained in parallel at any q-value.

EDXD measurements were performed upon a set of films. At first, a diffraction pattern of the substrate was collected to choose the ideal scattering angle in order to explore the q-range of interest and assign the substrate peaks, as shown in Fig. 1. The optimized working conditions were E=55 keV, I=20 mA and a scattering angle 2ϑ=14°. This preliminary set up was chosen to perform all the diffraction measurements and to collect the RCs of four different films: TiC, ZrC, HfC, and TaC.

Table 2
Results of the rocking curve analysis

	FWHM (degrees) [220]	FWHM (degrees) [331]
HfC	1.62±0.05	1.70±0.05
ZrC	1.22±0.05	1.38±0.05

The mean value of FWHM, deduced by the Gaussian fit, gives the estimation of the epitaxy index.
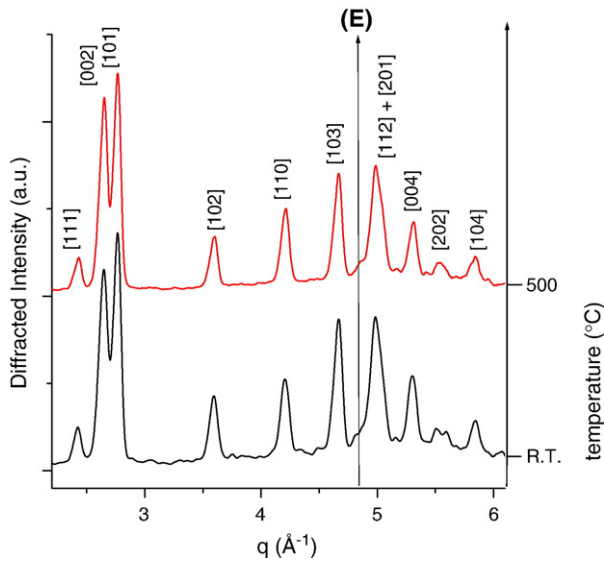
Fig. 5. Diffraction patterns of TiC/Ti, deposited at RT and 500 °C. The Ti reflections are labelled as before. The arrow (E) indicates the position of the TiC [331] reflection at $q=4.845$ (5) Å^{-1}.

The following measurements of the film-on-substrate system consisted of positioning the sample in the optical centre of the diffractometer upon a rotating cradle and maximize the diffracted intensity, which is mainly due to the substrate, scanning the asymmetry parameter α. The α position corresponding to the maximum intensity was set as $\alpha=0$. Starting from this position, the rocking curve was acquired by progressively increasing the asymmetry angle ($-2.5°<\alpha<2.5°$) while keeping the overall scattering angle unchanged.

2.3. Vickers hardness measurement

The hardness of the composite film/substrate system was measured with a Leica VMHT apparatus equipped with a
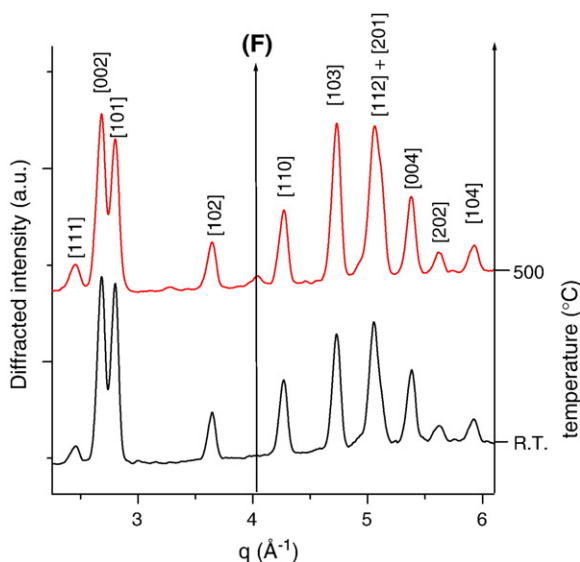
Fig. 6. Diffraction patterns of TaC/Ti, deposited at RT and 500 °C. The arrow (F) indicates the position of the TaC [220] reflection at $q=4.042$ (5) Å^{-1}.

standard Vickers pyramidal indenter. The loading and unloading speed was $5\cdot10^{-6}$ m/s, time under the peak load being 15 s. Indentations were made with 5 loads ranging from 0.098 to 19.6 N. To separate the hardness, H_c, of the film/substrate system on its constituents from the film (H_f) and the substrate (H_s), a Jönsson and Hogmark model based on an area law-of-mixture approach was used [17]. Furthermore, the indentation size effect was taken into account [18,19]. The reasonable expression for the H_c in this case is

$$H_c = H_{s0} + [B_s + 2ct(H_{f0} - H_{s0})]/D \qquad (1)$$

where $c \cong 0.5$ for brittle hard film on a more ductile substrate [17]; H_{s0} and H_{f0} are intrinsic hardness of substrate and film, respectively; t is film thickness; D is imprint diagonal, and B_s is the coefficient that can be determined from a separate experiment on the hardness of substrate. To calculate the intrinsic hardness of the film, special attention was paid to choose the indentation depths, d, correctly, i.e. in the interval where the model is adequate. According to the estimations, the d/t ratio must be in the range from >1 to 5 when the film is fractured conforming to the plastically deformed substrate [20]. Over this range of d/t, the results obtained by use of the Jönsson and Hogmark model has been demonstrated to coincide well with those resulting from more complicated approaches (Korsunsky et al., Chicot-Lessage) [21].

3. Results and discussion

SEM micrographs of films are shown in Fig. 2. The films are smooth and compact, with only few droplets on the surface (Fig. 2,a). The cross-sectional SEM observation showed no columnar structure (Fig. 2,b). The films consisted of nanoparticles of tens nanometers size approximately (Fig. 2,b, c, d) estimated from the SEM micrographs, the particle size being generally independent on the substrate temperature (room temperature or 500 °C). Averaged thickness of the films is given in Table 1.

The EDXD diffraction patterns of HfC films deposited on Ti at room temperature (RT) and at 500 °C are shown in Fig. 3. The
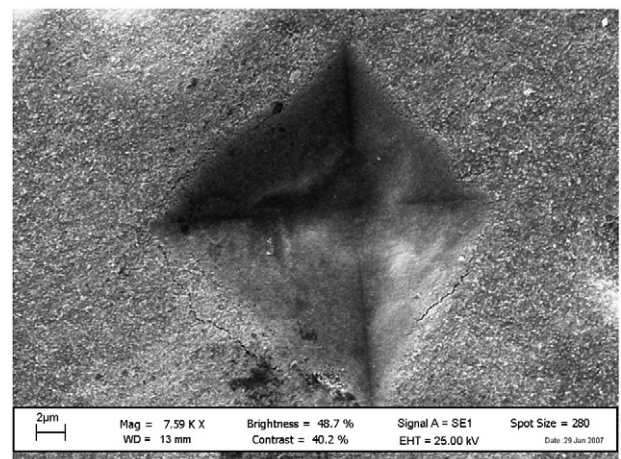
Fig. 7. SEM micrograph of an imprint of the indent on the surface of the ZrC/Ti composite system.

patterns were collected in the experimental conditions reported above and, by comparison with the pattern of the substrate only, it can be observed that all the Ti reflections are present. Two more Bragg peaks are visible and can be attributed to the film, being the HfC [220] reflection at $q=3.835$ (5) Å^{-1} (Fig. 3, arrow A) and the [311] at $q=4.495$ (5) Å^{-1} (Fig. 3, arrow B). To evaluate the epitaxial growth along these two directions, and to check if other reflections might be visible at a certain degree of the asymmetry angle, the RC analysis was performed in the range $-1.50°<\alpha<1.50°$. The results are shown in the inset of Fig. 3, where the rocking curves of the Bragg reflections (A) and (B), which are found to be the only crystalline growth directions of the material, are plotted. The RCs are fitted by Gaussian curves and the FWHM (Full Width Half Maximum), corresponding to the degree of epitaxy, were deduced. Moreover, through the angular α-displacement between the two maxima of the corresponding RC α_0 [220] and α_0 [331], the mismatch between these crystalline orientations is obtained ($\triangle\alpha=0.20°$).

The diffraction patterns of two ZrC films deposited on Ti at room temperature and 500 °C respectively, are shown in Fig. 4.

The diffraction peaks of the two substrates overlap perfectly. In the overall diffraction pattern, two more Bragg peaks are visible and can be attributed to the film. They correspond to the ZrC [220] reflection at $q=3.799$ (5) Å^{-1} (Fig. 4, arrow C) and to the [311] at $q=4.460$ (5) Å^{-1} (Fig. 4, arrow D). These reflections are present in both samples, regardless the deposition temperature and both the peaks shapes and intensities are comparable. Moreover, to evaluate the epitaxial growth along these two directions, the rocking curve analysis was performed in the angular range ($-3°<\alpha<3°$). The RCs relative to the ZrC <220> (C) and <311> (D) orientations grown at room temperature are shown in the inset of Fig. 4, being the only crystalline growth directions of the material. By the Gaussian fit of the curves, the FWHM were deduced and reported in Table 2, the degree of epitaxy being higher if compared to the same orientations in the HfC sample.

However, the mismatch between these crystalline orientations ($\triangle\alpha=0.51°$) is higher in the ZrC sample. When the ZrC film is grown at 500 °C, its crystalline reflections are still present and their intensities are higher than in the sample deposited at RT. However, a flat rocking curve is obtained for
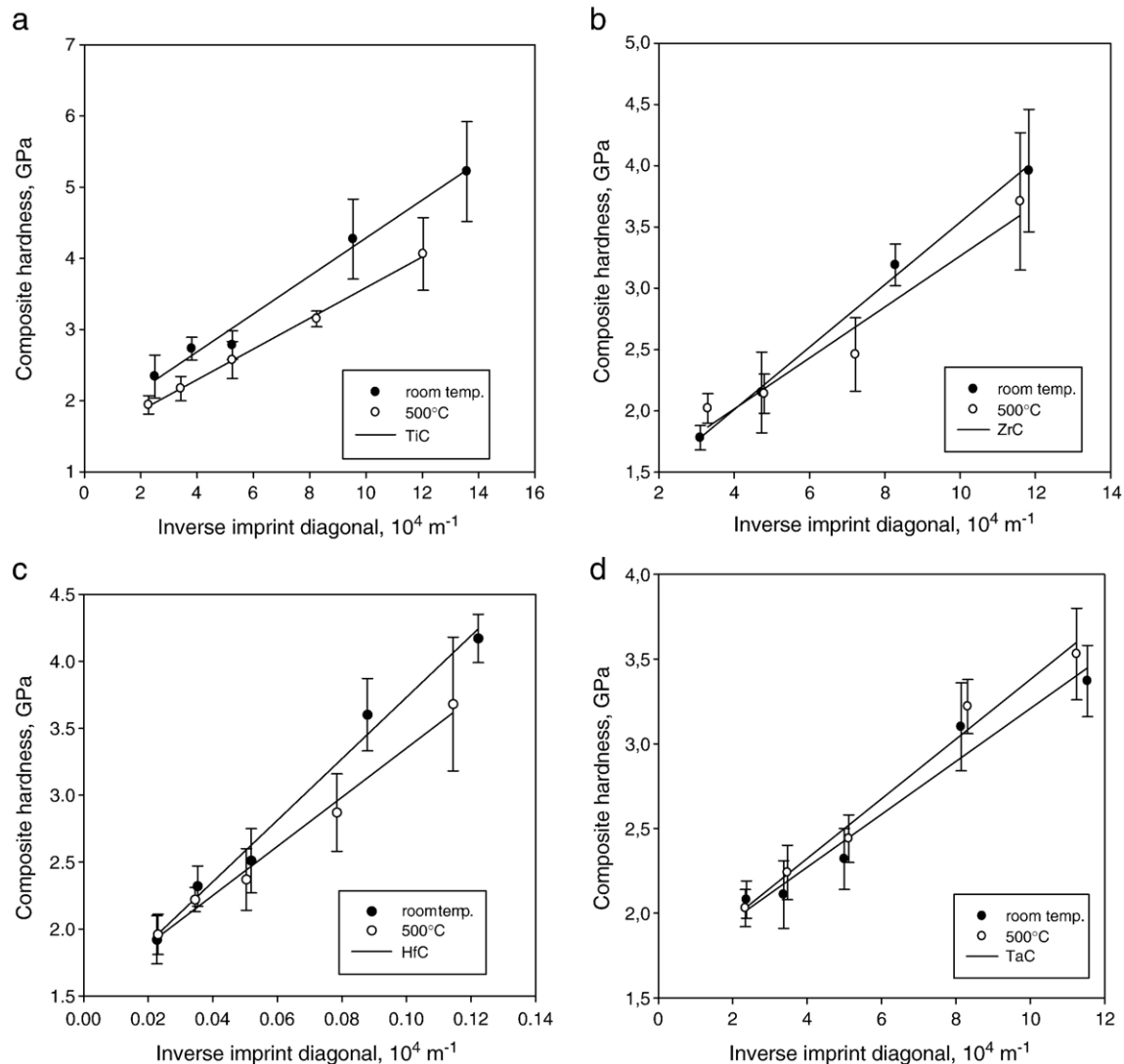
Fig. 8. Composite hardness of the film/substrate system versus inverse imprint diagonal: (a) TiC; (b) ZrC; (c) HfC; (d) TaC.

both the <220> and the <311> Bragg peaks. This evidences that a higher number of crystalline grains have grown within the film texture, but due to the temperature (500 °C) their orientation is completely disordered.

Diffraction patterns of a couples of TiC films deposited on Ti at RT and 500 °C, were collected in the same way as described above. In Fig. 5, the EDXD spectra are shown. Regardless of the deposition temperature, only a weak signal coming from the film is detectable. It corresponds to the TiC [331] reflection at $q=4.845$ (5) Å^{-1} (E), which is convolved with the much stronger reflections Ti [112] and [201], whose baricentral value is $q=5.060$ (5) Å^{-1}. As already mentioned, being the substrate polycrystalline, such strong reflection cannot be suppressed by tilting the sample, and, therefore, the film signal cannot be isolated. As a consequence, no information about the degree of epitaxy could be obtained. Nevertheless, the RC measurement excluded the presence of other detectable reflections, in the angular range $-2.50° < \alpha < 2.50°$.

The same experimental procedure was applied to a couple of TaC films, whose diffraction patterns are reported on Fig. 6. In this case, differences between the spectra collected at RT and 500 °C are visible. Indeed, in the former pattern, only the substrate signals are detected, no film reflection being visible. However, in the latter, the TaC [220] peak at $q=4.042$ (5) Å^{-1} can be observed (F). Concerning the TaC [331] Bragg peak, instead, it could not be detected. Therefore, if present, it is hidden by the substrate, no RC analysis being able to reveal it.

Thus, the EDXD data indicate the refractory carbides PLAD films grow with preferable orientations, and the grains orientation becomes random as the substrate preheating temperature is increased.

Fig. 7 shows an imprint of the indent on the surface of the ZrC/Ti composite system. The circumferential through-thickness fracture of the film is evident. Shown in Fig. 8 are the experimental plots H_c versus $1/D$ for all the coated samples. The plots were approximated well by a linear regression. A least-squares fit of the plots to the Eq. (1) results in the slope $B_c = B_s + 2ct(H_{f0} - H_{s0})$. Calculated intrinsic hardness values for

the films under study and the respective bulk carbide ceramics (data from Ref. [22]) are given in Table 1. Shown in Fig. 9 is the plot of film hardness versus molecular weight of carbides.

The following conclusions can be drawn from those data. Firstly, the hardness of the films is close to that of bulk ceramics, excepting for the hardness of TiC film which is somewhat lowered compared to that of the ceramics. The lowered hardness values cannot be the result from the invalid measurement technique, because the method has been proved by many studies (e.g. [10–12,17,23,24]). One possible reason is the diffusion of carbon from the film into the metallic titanium, as it has been revealed for electron beam deposited titanium carbide film on Ti substrate [25]. Indeed, a decrease in carbon content is known to lower the hardness of refractory carbides of the IV group of elements (TiC, ZrC, HfC) [22]. The diffusion rate rises with an increase in the substrate preheating temperature. However, the hardness of refractory carbides of the V group of elements (NbC, TaC) is known to decrease with an increase of carbon-to-metal ratio from 0.8 to 1.0 [22]. Hence, there are two opposing tendencies in effect of stoichiometry on hardness of the carbides of IV and V group metals. An increased hardness for the TaC film deposited at 500 °C has not been revealed, therefore the carbon diffusion cannot be considered as the main reason for the hardness value variation with the substrate temperature, at least for ZrC, HfC and TaC. The activation energy of carbon self-diffusion in these carbides (473, 545 and 497 kJ/mol, respectively) is significantly higher than in TiC (399 kJ/mol) [22].

Other possible reason is supposed to be the structural changes or alteration in the PLAD process and, consequently, in the microstructure development in the film. The disordered texture of the film deposited at elevated temperature was revealed by the EDXD rocking curve analysis. According to the results of a kinetic Monte Carlo simulation [13], the behavior of PLAD at a relatively low substrate temperature, i.e. at RT, is similar to that of molecular-beam epitaxy, which can result in textured microstructure. As the substrate temperature increases, there could be a crossover to PLAD which is markedly different from epitaxy, and the film growth mechanism is characterized by an increase in the island density.

The substrate temperature can affect the residual stress, microstructural features and hence the hardness of the film. Actually all vacuum-deposited coatings are in a state of stress [28]. The total stress is composed of a thermal stress and a so-called intrinsic stress. The first is due to the difference in the thermal expansion coefficients of the coating and substrate materials. The expansion coefficient of titanium is higher than that of carbides, so the compressive stress could be imposed on the film during the cooling of the coated system from 500 °C to RT. This stress might hinder the indenter penetration increasing the measured hardness value. The intrinsic stress is due to the accumulating effect of the crystallographic flaws during the deposition. The intrinsic stress in vacuum-deposited films of high melting point materials is almost exclusively tensile [28], resulting in lowered hardness. By means of the EDXD technique employed in the study it was impossible to evaluate a state of stress in the PLAD films because of a minimal q-shift within the
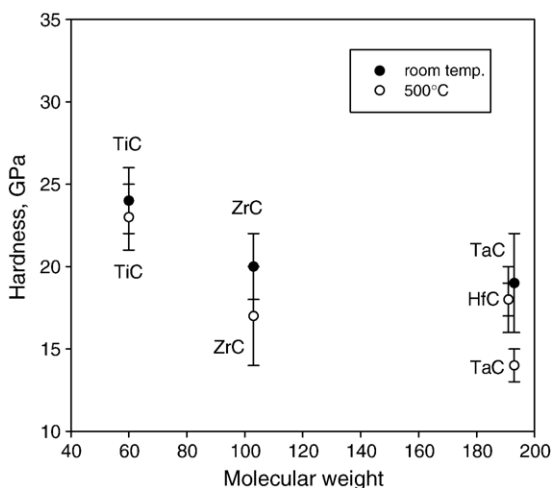
Fig. 9. Dependence of intrinsic film hardness on molecular weight of carbides.

experimental uncertainty attributed to the scattering parameter, is due to the electronic instabilities associated to the Energy Dispersive Mode which are in this shift range. This effect is more evident when broad peaks with an irregular shape are concerned. The intrinsic stress in the film deposited on preheated substrate can partially be relaxed due to recovery process. However, the substrate preheating temperature of 500 °C seems to be too low for the particle growth by recrystallisation process in the high melting point refractory carbides. SEM observation did not reveal any difference in the microstructure of films deposited at RT and at 500 °C. Thus, many factors can affect the hardness of the PLAD films of refractory carbides, and a further study is needed to individuate their contribution using additional experimental techniques, such as transmission electron microscopy, electron diffraction, X-ray photoelectron spectroscopy.

The hardness of the films decreases generally with an increase in the molar weight of the carbide, the trend being general for all refractory carbides of cubic structure belonging to the *Fm3m* space group [22,26]. The trend can formally be described by well-known Nowotny's equation: $H = k(T_m - T)/MV^{2/3}$, where k is a constant; T_m is melting temperature; V is molar volume, and M is molecular weight [27].

4. Conclusions

Thin films of titanium, zirconium, hafnium and tantalum carbides were deposited on titanium substrate by pulsed laser ablation method at the laser beam fluence of approximately 3 J/cm². Films are smooth and compact, their thickness is over the range from 220 to 600 nm. The films are nanostructured, the particle size being of tens nanometers approximately. The EDXD rocking curve analysis revealed the films are textured having preferable crystallographic orientation for growth. An increase of the substrate preheating temperature up to 500 °C results in a partial disordering of the texture and in a lowered hardness of the films. Hardness of the ZrC, HfC and TaC films is close to that of bulk ceramics, whereas hardness of TiC film is somewhat lower than that of bulk TiC ceramics, probably due to carbon diffusion from the film to the metallic substrate. Generally hardness of the films decreases with an increase of molecular weight of carbides.

References

[1] M. Long, H.J. Rack, Biomaterials 19 (1998) 1621.
[2] C.O. Freeman, I.M. Brook, J. Mater. Sci., Mater. Med. 17 (2006) 465.
[3] Y. Yang, K.-H. Kim, J.L. Ong, Biomaterials 26 (2005) 327.
[4] F. Fazan, P.M. Marquis, J. Mater. Sci., Mater. Med. 11 (2000) 787.
[5] S.C. Mishraa, B.B. Nayakb, B.C. Mohantyb, B. Millsc, J. Mater. Process. Technol. 132 (2003) 143.
[6] M. Brama, N. Rhodes, J. Hunt, A. Ricci, R. Teghil, S. Miglaccio, C. Della Rocca, S. Leccisotti, A. Lioi, M. Scandurra, G. De Maria, D. Ferro, F. Pu, G. Panzini, L. Politi, R. Scandurra, Biomaterials 28 (2007) 595.
[7] U. Sen, Thin Solid Films 483 (2005) 152.
[8] D. Ferro, S.M. Barinov, J.V. Rau, A. Latini, R. Scandurra, B. Brunetti, Surf. Coat. Technol. 200 (2006) 4701.
[9] A. Bendavid, P.J. Martin, T.J. Kinder, E.W. Preston, Surf. Coat. Technol. 163–164 (2003) 347.
[10] R. Teghil, A. Santagata, M. Zaccagnino, S.M. Barinov, V. Marotta, G. De Maria, Surf. Coat. Technol. 151–152 (2002) 531.
[11] G. De Maria, D. Ferro, L. D'Alessio, R. Teghil, S.M. Barinov, J. Mater. Sci. 36 (2001) 929.
[12] S.M. Barinov, D. Ferro, C. Bartuli, L. D'Alessio, J. Mater. Sci. Lett. 20 (2001) 1485.
[13] X. Tan, Y.C. Zhou, X.J. Zheng, Surf. Coat. Technol. 197 (2005) 288.
[14] R. Teghil, L. D'Alessio, A. Santagata, M. Zaccagnino, D. Ferro, D.J. Sordelet, Appl. Surf. Sci. 210 (2003) 307.
[15] R. Caminiti, V. Rossi Albertini, Int. Rev. Phys. Chem. 18 (1999) 263.
[16] B. Paci, A. Generosi, V. Rossi Albertini, E. Agostinelli, G. Varvaro, D. Fiorani, Chem. Mater. 16 (2004) 292.
[17] B. Jönsson, S. Hogmark, Thin Solid Films 114 (1984) 257.
[18] A. Iost, R. Bigot, Surf. Coat. Technol. 80 (1996) 117.
[19] F. Fröhlich, P. Grau, W. Grellman, Phys. Status Solidi A 42 (1977) 79.
[20] A.M. Korsunsky, M.R. McGurk, S.J. Bull, T.F. Page, Surf. Coat. Technol. 99 (1998) 171.
[21] E.S. Puchi-Cabrera, Surf. Coat. Technol. 160 (2002) 177.
[22] R.A. Andrievski, I.I. Spivak, Strength of Refractory Compounds and Related Materials, Metallurgy, Tcheljabinsk, 1989.
[23] V. Natravil, V. Stejskalova, Phys. Status Solidi A 157 (1996) 339.
[24] D. Ferro, R. Teghil, S.M. Barinov, L. D'Alessio, G. De Maria, Mater. Chem. Phys. 87 (2004) 233.
[25] D. Ferro, R. Scandurra, A. Latini, J.V. Rau, S.M. Barinov, J. Mater. Sci. 39 (2004) 329.
[26] A. Krajewski, L. D'Alessio, G. De Maria, Cryst. Res. Technol. 33 (1998) 34.
[27] H. O'Neill, Hardness Measurements of Metals and Alloys, Chapman&-Hall, London, 1967.
[28] J.E. Thornton, D.W. Hoffman, Thin Solid Films 171 (1989) 5.